

称号及び氏名 博士(理学) Jean-Baptiste HARLE

学位授与の日付 平成 29 年 12 月 31 日

論文名 Streptocyanine Dyes for Dye-Sensitized Solar Cells: Design,
Syntheses, Optoelectronic Characterizations and Persistence
at the Electrolyte/Dye/TiO₂ Interface
(色素増感太陽電池のためのストレプトシアニン色素:分子設計、合
成、光電子的評価と電解液/色素/酸化チタン界面における安定
性)

論文審査委員 主査 藤原 秀紀
副査 松坂 裕之
副査 神川 憲
副査 松原 浩

論文名: **Streptocyanine Dyes for Dye-Sensitized Solar Cells: Design, Syntheses, Optoelectronic Characterizations and Persistence at the Electrolyte/Dye/TiO₂ Interface.**

(色素増感太陽電池のためのストレプトシアニン色素：分子設計、合成、光電子的評価と電解液／色素／酸化チタン界面における安定性)

Abstract of Ph. D Thesis

Jean-Baptiste HARLE

Chapter 1 is an *Introduction to Photovoltaics* that explains the background and general purpose of this study: A first essentialization of actual climate paradigms and a brief contextualization of the development of renewables and clean energies in the light of today's watershed in energy productions are summarized. Then, the thesis focuses on the Dye-sensitized solar cell (DSSC) amidst existing solar technologies, and depicts in details each working mechanism within the cell before offering a glimpse at the pioneering and state-of-the-art dye-sensitizers.

Dye-sensitized solar cell has attracted lots of interests since the publication of Michael Grätzel and Brian O'Regan in *Nature* 1991. The device, working on the I₃⁻/I⁻ electrolyte as liquid redox shuttle, mesoporous TiO₂ anatase as electron collector and a Ruthenium-based sensitizer harvesting sunlight, stabilized at the interface. Such a device exhibited ~11% conversion efficiency (η) under AM1.5 (Global Air Mass 1.5) one sun illumination. Since then, miscellaneous components have been reported for the technology, and the 12% efficiency threshold was surpassed with zinc porphyrin-based sensitizers and the less corrosive tris(2,2'-bipyridyl)Cobalt(II/III) one-electron redox shuttle. A zinc/cobalt-based technology would allow wide-scale perspectives for the technology compared to ruthenium, but in both cases the sensitizers require complicated syntheses and tricky purification steps, limiting synthetic versatility and industrial perspectives. However, the Donor- π -Acceptor (D- π -A) and similar motifs of full organic sensitizers offer several advantages over metal-centered ones, such as better light absorption, facile tuning of the ground and excited energy levels and building thanks to worthwhile, easily scaled-up synthetic routes. Many dye designs have been investigated and reported and displayed quantitative conversion efficiencies over a part of the visible spectra, at wavelengths well below 700 nm up so far. The Shockley-Queisser limit for single junction devices shows a theoretical best 33% conversion limit for a

device with a bandgap around 1.1 ~1.2 eV, corresponding to a max wavelength around 1100 nm. Further limitations arise from thermodynamic losses due to the conversion process: the 0.2 eV necessary driving force for quantitative electron injection, the cost for recombination between the dye and the redox mediator and the overpotential due to regeneration of this very mediator at the back contact. Considering these limitations, a large share of the far red/ Near-IR solar spectra remains available and the race toward efficient sensitization at these wavelengths is strikingly difficult and most often requires elaborated and complex structures, longer π -conjugation and insertion and heavy heteroatoms. The most famous examples of metal-free low band gap chromophores already reported efficient for sensitization at longer wavelength are closed-chain-, hemi- and streptocyanines, Pechmann (diketopyrrolopyrrole) dyes, and remain really scarce in the literature with the exception of squaraine dyes. Among these, the most readily accessible are unequivocally the cyanine-functionalized, first discovered back in 1856 by C. H. Greville Williams, already reported available for DSSCs and to the design and stabilization of which I devoted most of the time that was allotted to me for this PhD course.

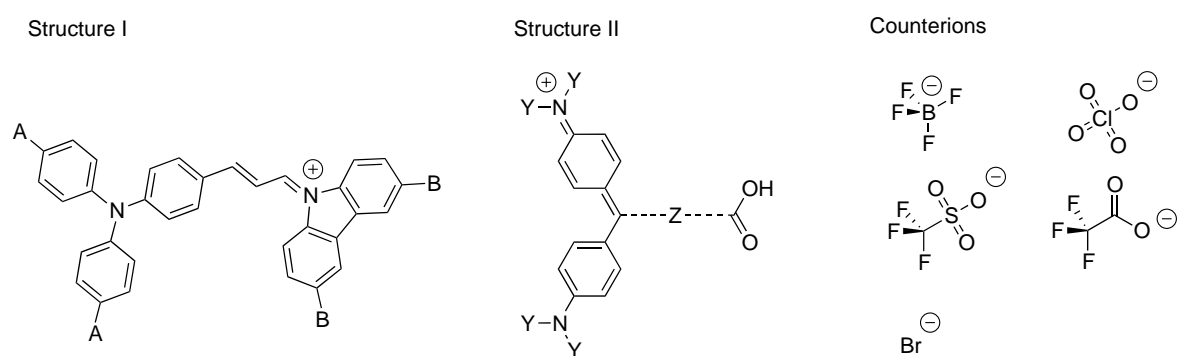


Figure 1. Structures of the streptocyanine dyes of cationic structures **I** with A = H, OHex and B = H, OMe, OH and **II** with Y = *p*-OMePh, *p*-OHexPh, *n*-Dec, Me and Z = 1,4-phenyl (Ph) and 2,5-thienyl (Th) and their counterions tetrafluoroborate (BF_4^-), bromide (Br^-), triflate (TfO^-), trifluoroacetate (TFA^-) and perchlorate (ClO_4^-).

Chapter 2 describes a study entitled *Asymmetrical Carbazolium-based Streptocyanines* on the characterization and the counterion-specific stabilization of carbazolium-based streptocyanine dyes designed for DSSC use. The dyes merely consisted in an ionic pair, the cationic part being the cyanine chromophore, conjugated to a given counterion transparent to visible light. The newly developed substituted dyes, of structures (*E*)-[(diphenyl-amino)phenyl]allylidene-

carbazolium (**I**) with various substituents (**1H**⁺: A = H, B = H; **1OMe**⁺: A = H, B = OMe; **1OH**⁺: A = H, B = OH; **2OH**⁺, A = O-Hex, B = OH) and counterions (triflate (TfO⁻), tetrafluoroborate (BF₄⁻) and perchlorate (ClO₄⁻)) were developed and their UV-vis and optoelectronic properties were characterized (**Figure 1**). Furthermore, the anchoring-capable dyes **1OH**⁺ and **2OH**⁺ were successfully integrated in dye-sensitized solar cells. The dyes displayed different dielectric behaviors as a function of the nature of their counterion: the adsorption potential of the counterions had a large bearing on the stability of the chromophores at the electrolyte/dye/TiO₂ interface. Typically, they sharply altered their affinity for the surface / affinity for the bulk ratios in DSSC conditions, ca. in highly concentrated ionic media. The affinity of the TfO⁻ and ClO₄⁻ counterions for the surface thermodynamically compensated for the loss of entropy undergone by the small cationic π -systems when adsorbed onto titania and prevented its diffusion away from: after 5 seconds in a standard I₃⁻/I⁻ DSSC electrolyte, the dyes **1OH-TfO**, **2OH-TfO** and **1OH-ClO₄** desorbed by 5%, 7% and 26%, respectively, while **1OH-BF₄** desorbed by 54% (**Figure 2**). This characterized coadsorption of both the chromophoric cation and its counterion improved the properties and stability of the carbazolium-based dyes (structure **I**) at the surface of TiO₂ in Grätzel cells, and consistent with the zeta potential values of colloidal suspensions of sensitized nanoparticles. The results indicated a large excess of BF₄⁻ ($\zeta_{1OH-BF_4} = -18.24$) in the diffuse layer and a near equivalence of the ionic distributions with respect to the distance to the surface in the case where both the chromophore and its counterion are anchored at the surface, cancelling the zeta potential values ($\zeta_{1OH-TfO} = +0.49$, $\zeta_{1OH-ClO_4} = -1.26$, $\zeta_{2OH-TfO} = +0.34$). The electric potential gradients for both cases are depicted in Figure 2, middle and right.

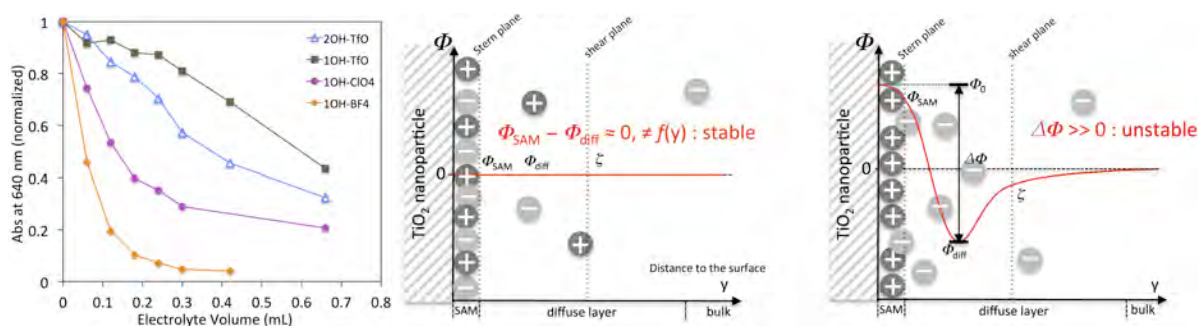


Figure 2. *left:* Desorption of the dyes **2OH-TfO**, **1OH-TfO**, **1OH-ClO₄**, **1OH-BF₄** from TiO₂ nanoparticles when dipped in an electrolyte containing 0.5 M DMPII, 0.14 M LiI and 0.04 M I₂ in dry acetonitrile. The absorbance at 640 nm was normalized with respect to the initial absorption value (V = 0 mL) and plotted as a function of volume of electrolyte (mL). Modeling of the ionic distributions at the surface in a semi-infinite

domain for (*middle*) TiO_2 coadsorbed cations and anions with equivalent distribution at - and proximate to the surface and (*right*) cations adsorbed at the TiO_2 surface and free anions. The electric potential Φ is illustrated as function of the distance to the surface y and equal to Φ_{SAM} at the Stern plane at the limit of the self-assembled monolayer, to Φ_{diff} at the barycenter of the negative charges in the diffuse layer and to the ζ potential at the shear plane. $\Delta\Phi$ is the difference between the barycenter of the positive charge Φ_0 and the barycenter of the negative charge Φ_{diff} .

Put in perspective with the conversion efficiencies (η) and the cells parameters, one can observe that the properties of the solar cells highly depended on the nature of the counterion. With a conversion offset around 850 nm (**Figure 3, right**), the cells converted sunlight over the whole visible spectrum and the best conversion efficiency was obtained with the O-Hexyl-substituted **2OH-TfO** with 1.08%. Interestingly, the conversion of **1OH**⁺ dropped by as much as 28% when replacing the coadsorbed triflate counterion by the free tetrafluoroborate, owing to a lower fill factor ($ff(\mathbf{1OH-TfO}) = 0.53$; $ff(\mathbf{1OH-BF}_4) = 0.40$). The free counterion not only altered the stability of the grafting of the dye at the $\text{TiO}_2/\text{dye}/\text{electrolyte}$ interface but also deteriorated the device's capacities.

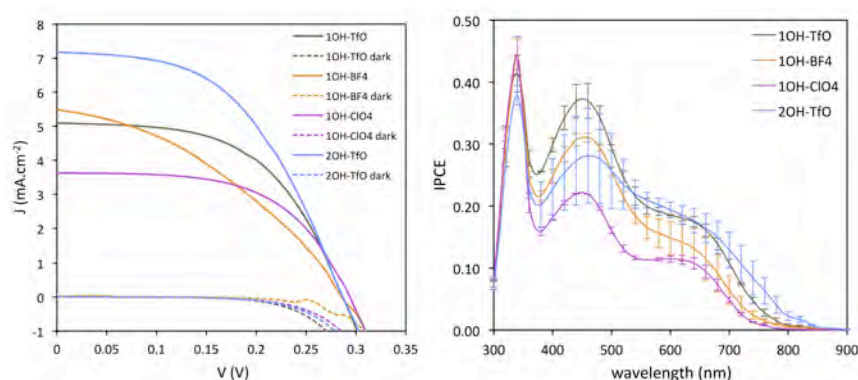


Figure 3. Photocurrent-voltage characteristics curves (*left*) and IPCE action spectra (*right*) under AM 1.5 artificial sunlight source for nanocrystalline TiO_2 solar cells sensitized with **1OH-TfO** (brown), **1OH-BF₄** (orange), **1OH-CfO₄** (purple) and **2OH-TfO** (blue) dyes. The error bars in the IPCE spectra correspond to the standard deviation of the measurements of two solar cells measured under identical conditions.

Chapter 3 describes a study entitled *Malachite Green Derivatives*. The derivatives, named after the brilliant green malachite green dye and of structure **II** were developed for DSSC use. The chromophores **3Me**⁺ (Y = Me, Z = Ph), **3Dec**⁺ (Y = *n*-Decyl, Z = Ph) and **4Me**⁺ (Y = Me, Z = Th) displayed a maximum absorption around 630–650 nm in solution, corresponding to the lowest energy transitions (HOMO-LUMO), with orbital coefficients similar to those of Malachite Green (**Figure 4**).

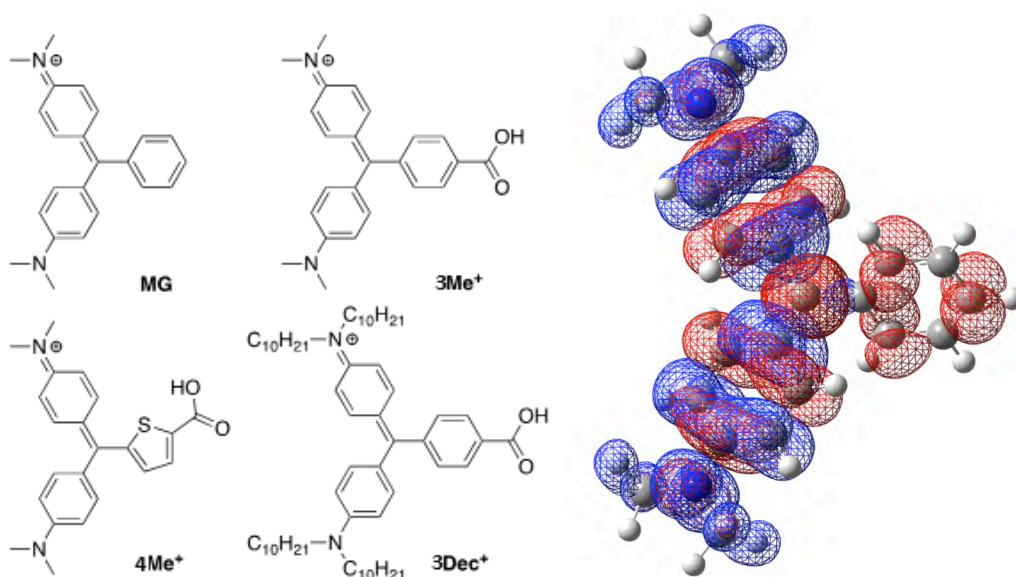


Figure 4. *left:* Chemical structures of malachite green (**MG**) and its derivatives **3Me⁺**, **4Me⁺** and **3Dec⁺** developed for the present study and represented in their quinonoidal form. *right:* Optimized structure of Malachite Green: front view of the HOMO (blue) and LUMO (red) isodensities, computed by DFT calculations with B3LYP 6-31G** basis set.

Adsorbed at the surface with a common lone carboxylic acid, the cationic dyes displayed a high dependency to their dielectric environment: Co-stabilization of the counterion at the surface shattered the series and shunt resistances, fill factors and thus V_{MAX} , J_{MAX} , and the photovoltaic conversions thereof: **3Me⁺** showed the best photoconversion efficiencies, owing to its higher lying LUMO level (-0.47 V vs NHE) and best sensitized the cell with TFA⁻ as counterion ($\eta = 0.37\%$). The V_{OC} increased with J_{SC} and the electron current density (**Figure 5, left**) The efficiency then dropped to 0.22% with BF₄⁻, 0.14% with Br⁻ and 0.13% with TfO⁻. A better photovoltage could be achieved, altogether with better fill factors, with the malachite green derivatives thanks to a lower lying ground state redox level that allowed sensitization of the photoanode in combination with a Br₃⁻/Br⁻ electrolyte ($E^0(\text{Br}_3^-/\text{Br}^-) = +1.09$ V vs NHE) used instead of the standard I₃⁻/I⁻ shuttle. This work was an attempt at qualitatively disentangling, through experimental characterizations, every contribution of (i) the electric double layer patterns at the surface and (ii) the counterions' nature on both the efficiency of the device and stability of the dye at the surface. The excess species in the diffuse layers of sensitized nanoparticles in colloidal solutions were characterized by zeta potential measurements and successfully compared to the desorption patterns of the dyes. The likelihood that the reported behavior of these dyes might be extended to any cationic dye is

high, and could thereby help assessing anchoring instability issues and at the same time boosting their photoconversion yields.

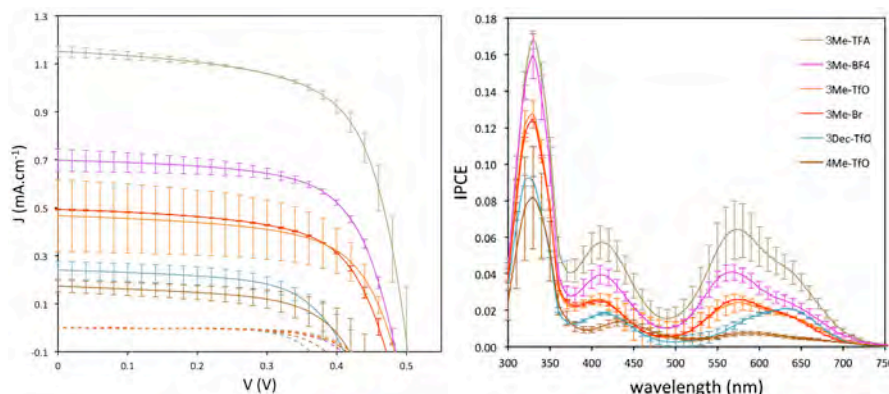


Figure 5. *left:* Photocurrent (J) -voltage (V) characteristics curves under AM 1.5 artificial sunlight source (plain) and dark conditions (dotted line) and *right:* IPCE action spectra for nanocrystalline TiO₂ solar cells sensitized under argon with the dye sensitizers dipped in 1.00 M LiBr(H₂O) / 0.05 M Br₂ in superdry CH₃CN. The error bars represent the standard deviation on the measurements obtained with at least two cells prepared under the very same condition. No further additives were used in the electrolyte.

Chapter 4 describes the general conclusions of the researches.

List of publications:

- 1) Deep blue asymmetrical streptocyanine dyes: synthesis, spectroscopic characterizations, and ion-specific cooperative adsorption at the surface of TiO₂ anatase nanoparticles, Harlé, J. -B.; Mine, S.; Kamegawa, T.; Nguyen, V. T.; Maeda, T.; Nakazumi, H. Fujiwara, H., *J. Phys. Chem. C*, *121*, 15049-15062 (2017)
- 2) Malachite green derivatives for dye-sensitized solar cells: optoelectronic properties and persistence on TiO₂, Harlé, J. -B.; Arata, S.; Mine, S.; Kamegawa, T.; Nguyen, V. T.; Maeda, T.; Nakazumi, H.; Fujiwara, H., *Bull. Chem. Soc. Jpn.*, *91*, 52-64 (2018)

学位論文審査結果の要旨

色素増感太陽電池(DSSC)は、色素分子を酸化チタンに吸着させ、電解質溶液を添加したセル構造を有しており、その廉価性、容易な製造方法、高い変換効率から注目を集めている。その中で、レアメタルフリーな D- π -A 型色素分子が、合成が容易で高い吸光係数を有し、分子設計によるオービタル準位の微調整が可能なことなどから多くの研究がなされている。中でも太陽光エネルギーの有効活用のためには、近赤外光の利用が重要な課題となっているが、本研究では、600~700 nm の長波長域に強い光吸収を示す各種ストレプトシアニン色素について、DSSC に適用可能な分子修飾を施すとともにその分子・電子構造、光電子的物性を明らかにした。また、酸化チタン上でのカチオン性色素分子の吸脱着性や太陽電池性能に対する対イオンの影響を各種測定手法により解明した。その結果、以下に示す成果が得られた。

(i) 新規な非対称カルバゾリウム色素を合成した。その中で DSSC 用の吸着部位である水酸基を有する色素について、酸化チタン上での吸脱着性や太陽電池性能を評価したところ、 TfO^- のような酸化チタンに配位可能な対イオンの場合にはカチオン性色素の脱離が抑制され太陽電池性能も高く、逆に BF_4^- のように酸化チタンへの親和性が低い場合には、容易にカチオン性色素が酸化チタンから脱離し太陽電池性能も低くなることを見出した。このことから、本来光電変換に直接関わりを持たない対イオンが太陽電池性能に大きな影響を与えることを見出した。

(ii) DSSC 用マラカイトグリーン色素分子を簡便な方法により合成した。この色素は低い HOMO 準位を有するため、臭素レドックス対を用いることで、電池の開放電圧が大きく改善されることがわかった。また、(i) と同様に対イオンによって吸脱着性が大きく変化すると共に、酸化チタンに注入された電子の再結合過程にも対イオンが大きく関わっているため、両方の効果の競合により太陽電池性能が影響を受けることを見出した。

以上のように、本研究では DSSC 用の新規色素分子の開発と物性評価に成功するとともに、酸化チタン/電解液界面での色素分子の吸脱着と電池性能に関する対イオンの役割についての新たな重要な知見を与えた。よって学位論文審査委員会は本論文が学位論文として十分な内容を有しているものと判断し、博士(理学)の学位を授与することを適当と認める。

学位論文審査委員会

主査 藤原 秀紀
松坂 裕之
神川 憲
松原 浩